Reviewer 1 Report Rebuttal

Please find a point by point response to the referee's comments. N.B. the referee's comments are in blue and our responses are in black. We also upload a copy of the manuscript in which changes from the previous version are highlighted for the referee's convenience.

Reviewer 1

This manuscript investigates the impact that tip speed ratio (TSR; 7 different TSRs tested) and free-stream turbulence (FST; 3 different FSTs tested) have on both the strain acting on a wind turbine rotor blade, and the wake of that wind turbine. To investigate the edgewise and flap-wise strain response, a Rayleigh backscattering sensor (RBS) is integrated along the span of one rotor blade in a sinusoidal pattern that allows for simultaneous measurements at multiple positions along the blade.

Overall, while the manuscript is well written, and the presentation of this set-up is very interesting, there are many open questions and some potentially severe flaws in the presentation and interpretation of the results.

The Abstract and Conclusion should be updated according to the comments.

We appreciate the reviewer's thorough evaluation of our manuscript and valuable comments. We hope that the referee's concerns have been addressed in our revised manuscript.

The conclusions were also revised.

Note to the reviewer:

The reviewers' comments prompted us to undertake a thorough, "root-and-branch" reappraisal of the manuscript as a whole. Beyond the specific points raised, this process led us to identify a number of areas where the scientific content, clarity, and rigour of the paper could be improved. We have therefore introduced several additional modifications that were not explicitly requested but which we believe significantly raise the scientific quality of the manuscript.

We have added section 2.4., clearly detailing the experimental protocol followed, specifying the two independent tests conducted to produce the datasets presented. Section 3 has been reshaped completely. We have added section 3.2. to include data from the blade's response to a static unidirectional load case, where we have explored the effect of incremental loads on the blade, to assess how it reacted under 3 different loading cases. Section 3.3. refers to the blade loads under a quiescent background, and we have now added the spectra of the strain under 3 representative rotation conditions under these circumstances. The spectra of the strain under quiescent conditions are presented in figure 9, which also provides key evidence for the aerodynamic origin of the $St_\Omega = 3$ signature in the blade strain spectra. We have updated the notation for the decomposed strain components throughout the revised manuscript: what was previously referred to as *flapwise strain* (ε^f) is now denoted *spanwise strain* (ε^s), and *edgewise strain* (ε^e) is now referred to as *chordwise strain* (ε^c). This change more accurately reflects the geometry of the fibre-optic sensor layout, which is aligned with the blade's spanwise and chordwise axes in the blade coordinate system $s\mathcal{O}c$, rather than with the classical structural flapwise/edgewise decomposition. The flapwise and edgewise bending moments (M^f and M^e) are retained where they refer to structural mechanics. Section 7 was also added to exploit the concurrent measurements we conducted in $T1$, where we present cross-power spectral densities for representative test cases. We have also added the spanwise distributions of RMS(ε'_a) to figure 16 *a)* to complement the analogous distributions of time-averaged strain in figure 13. We have also added substantial material to the appendix for the benefit of clarity: appendix A details the homogeneity of the FST operating conditions across the span of the turbine; appendix B provides a detailed overview of uncertainty on the conducted hot-wire measurements, appendix C details the blade geometry used and aerofoil profiles chosen. Appendix D details the least-square detrending procedure used to correct strain

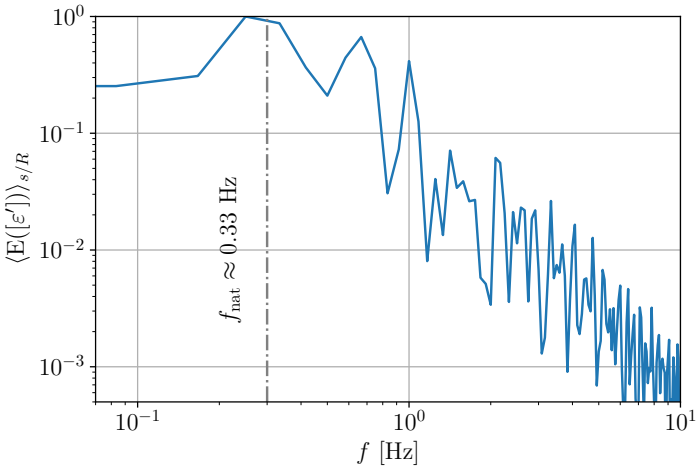

Figure 1: Spectrum of spanwise ensemble-averaged fluctuating strain ($\langle E([\varepsilon'])\rangle_{s/R}$) during free-decay test.

signal drift observed in $T1$. The chordwise time-averaged strain have been moved to appendix E, reported for completeness and transparency rather than as a well-characterised aerodynamic finding.

Major comments:

1. The resonance frequencies of the blades, the tower+nacelle, and the whole turbine are missing. Considering that strain fluctuations are the main focus of this study, this is crucial information to ensure that the effects are not due to resonance. Did you ensure (by measuring) that the turbine was not vibrating during the measurements?

   We thank the reviewer for pointing this out. A free-decay test was performed by exciting the instrumented blade at rest, and analysing the strain response measured across the blade. The resulting amplitude-normalised spectrum (presented here in figure 1 of the rebuttal) exhibits a dominant peak at $f \approx 0.33$Hz identified as the first natural frequency of the blade. Higher-frequency peaks correspond to higher-order modes with significantly lower energy. As the rotation frequencies (for the considered λ in this work) remain well separated from the identified blade's natural frequency, we assume the results are not contaminated by blade resonance. Arguably, the only case in which the rotational frequency approximates one of the blade's natural frequency harmonics is for $\lambda = 1$ where the rotational frequency is $f_{\mathrm{ROT}} \approx 0.98$Hz, and the $3rd$ harmonic of $3f_{\mathrm{nat}} \approx 1$Hz. If the blade resonance was to have an impact in the measured dynamics, $\lambda = 1$ would present an isolated case of increased energy/r.m.s. of ε', which is not the case as evidenced in the discussion. Therefore, we can assume that the influence of blade resonance was negligible in all results presented in the manuscript.

   As the tower+nacelle system are made out of thick aluminium, and particularly the tower is constructed from an aluminium bar (5mm of thickness and 50.8mm diameter), and bolted to a 38.1mm thick, and $600 \times 450\mathrm{mm}^2$ steel base, which was directly connected to the wind-tunnel floor. Given the large stiffness of this assembly, we expect its natural frequency to lie well above the frequency range of interest. Initial free-decay tests were conducted and RBS were used acquiring data at $f = 100$Hz to try and characterise the natural frequencies of the subsystems under consideration. The results were inconclusive both as a result of very low strain values with variations of $\approx 2\mu\varepsilon$, without any clear peaks on the spectra. Bearing this in mind, we can conclude that the natural frequency related to this system does not affect the results presented. This information has been added to the revised manuscript - see last paragraph of section 3.2.

2. One of the main aspects of this article is said to be the "coupled wind turbine blade/wake dynamics". For this, the hot-wire measurements and RBS measurements are synchronized, as described on pages 8 and 9. However, these measurements are not evaluated in a way that actually makes use of the synchronization -

the hot-wire measurements and strain measurements are analyzed separately to then draw conclusions on how the blade is affected by the wake. Without actual evidence, it is e.g. concluded that the $St = 3$ - mode of the blade strain is due to a back-coupling of the tip vortex structures in the wake of the turbine farther downstream. I am doubtful about this interpretation and would rather assume that the observations are due to stronger vibrations and variations in the rotational speed (the authors report small variations but that could still be sufficient to see harmonics) at higher turbulence intensities and TSRs. In a similar manner, I would assume that the strain fluctuations at the blade tip are highest because the blade profiles are thinnest and most flexible there.

We thank the reviewer for this important comment. We agree that, in the original version of the manuscript, the synchronisation between the hot-wire and RBS measurements was not fully exploited to provide direct evidence of coupled blade-wake dynamics. We originally left this out since we initially felt that inclusion of this data plus associated discussion would result in an overly long manuscript.

To make explicit use of the synchronised measurements, we have added a cross-power spectral density (CPSD) analysis between the fluctuating blade strain and the near-wake velocity fluctuations (new section 7, new Fig. 23). The CPSD provides a direct, frequency-resolved measure of statistically correlated dynamics between the two synchronised signals. The CPSD maps reveal narrow energetic bands at $St_\Omega \in \{1, 2, 3\}$. Particularly, the bands at $St_\Omega = 3$ show incerased energy in the near-wake shear layers, rather than along the wake centreline. This spatial structure of the cross-spectral-correlation supports the aerodynamic origin of the shared dynamics, and the coupling of blade dynamics to the tip-vortex system originating at the wake of the turbine. The emergence of $St_\Omega = 3$ coupled dynamics—a frequency signature absent from blade inertial mechanics but characteristic of the wake's tip vortical structure—provides evidence of directional causation: coherent wake motions are imprinted onto the blade response, likely through pressure fluctuations. The separation of the natural frequency of the blade to the range of frequencies of interest further strengthens this point.

Regarding the reviewer's concern that the observed $St_\Omega \approx 3$ strain component may arise from rotational-speed variability or increased structural flexibility at the blade tip, we note that such effects would be expected to produce rotor-harmonic content that is broadly distributed across the wake's transverse direction (y) and blade's spanwise extent. In contrast, the CPSD shows that the strongest shared dynamics are confined to the shear-layer regions associated with the tip and root vortex system, and that their magnitude depends systematically on operating condition and FST.

Moreover, while we do observe small variations in rotational speed ($\Delta\Omega \approx 9$rpm maximum at $\lambda = \lambda_d$), the frequency content of these motor-induced fluctuations is effectively decoupled from the blade dynamics due to the mechanical configuration. The motor is connected to the rotor through a 1:3 gear reduction. Furthermore, the motor's ESCON controller actuation is typically of a much higher frequency than its operating velocity—on the order of kHz–, as it adjusts the action to correct drifts from rotational speed with a fine-tuned PID control system. We ensured that this was not affecting our measurements. The gear ratio combined with the mechanical damping inherent in the gear system ensures that high-frequency motor dynamics are significantly attenuated before reaching the blade. Consequently, the motor-induced speed variations and aerodynamic strain fluctuations occur in largely separated frequency bands, addressing concerns about strong correlation between these components. This supports the interpretation of a coupled blade-wake system dominated by rotor-synchronous coherent structures, while remaining consistent with the possibility of common forcing rather than one-way causality.

The emergence of the $St_\Omega = 3$ signature in the blade strain spectra under "wind-on" conditions provides key evidence for its aerodynamic origin. Under quiescent background conditions, the strain spectra show negligible energy at $St_\Omega = 3$ across all tested tip-speed ratios, confirming that this frequency is not an artifact of the mechanical system, rotational forcing, or gravitational and centrifugal loading. We have now added this information to section 3.3. "Blade strain under gravitational and centrifugal loading". The peak emerges prominently only when the wind turbine is exposed to $U_\infty \neq 0$ m.s^{-1}, implicating an aerodynamic mechanism as its source by process of elimination. This is further corroborated by the cross-power spectral density analysis between concurrent wake velocity and blade strain measurements,

which confirms the presence of the same dominant frequency in both signals, establishing that the $St_\Omega = 3$ dynamics are part of the coupled wake-blade system.

The physical origin of this signature is consistent with the periodic encounter of the reference blade with the tip-vortex structures shed by the other two blades. In a three-bladed rotor, all three blades shed helical tip-vortex systems displaced in azimuth by 120°. Viewed from the rotating frame of any one reference blade, this three-fold symmetric vortex field is not aerodynamically steady: as the reference blade completes each revolution, it periodically encounters the pressure field associated with tip-vortex structures shed by the *other two* blades. This periodic encounter is further reinforced by the fact that tip vortices advect at a velocity smaller than the free-stream, causing them to bunch up as they propagate downstream and creating a spatially concentrated pressure field that is imprinted back onto the blade strain response at three times the rotational frequency. This aerodynamic mechanism is distinct from the gravitational and centrifugal contributions, which produce energy at $St_\Omega = 1$ and $St_\Omega = 2$ through the once-per-revolution and twice-per-revolution inertial forcing in the rotating frame. The clean separation of these spectral signatures, combined with their distinct behaviour under wind-on and wind-off conditions, supports the interpretation that the decomposition methodology successfully isolates the aerodynamic strain component from the inertial baseline. This discussion has been added to the last paragraph of section 6.1. of the revised manuscript, "Integrated Spectral Energy Across Frequencies".

The blade's tip profiles are indeed "thinner", and produce the largest RMS(ε') as observed in what is now figure 16 b), and on the uncertainty bars of the Δ_s in figure 15 of the revised version of the manuscript. We now clearly refer this in line 498 of the revised manuscript.

Overall, the revised manuscript now uses the synchronisation directly to demonstrate frequency-resolved coupling between blade strain and near-wake velocity fluctuations, and we explore more appropriately, by presenting evidence backed up by the spectra of "wind-off" strain data contrasting with the "wind-on" data, that $St_\Omega = 3$ is indeed of aerodynamic nature.

3. From the results presented here, I do not agree with the authors' direct conclusion that the wind turbine wake affects the blade dynamics - this to me seems like an indirect conclusion without the necessary proof, e.g. through correlating the two signals. In [11], for example, it is shown how the vibration-induced motion of a blade tip, through induced lift variations, the strength of the tip vortex (not the other way round). Alternatively, I can see a direct argumentation where the flow field around the profile (with all the structures that are shed) does impact the blade, but that does not explain the relation of the $St = 3$-mode to the tip vortex shedding of three blades.

   This is related to the discussion of the previous point 2.

   The intention of the manuscript is not to imply a unidirectional wake-to-structure forcing, but rather to demonstrate a statistically significant coupling between coherent wake dynamics and blade strain fluctuations. We provide two independent lines of evidence for this coupling. First, the CPSDs of the concurrent wake velocity and blade strain signals provide a frequency-resolved quantification of the statistical coupling between the two, confirming that coherent energy is shared between the wake and the blade at $St_\Omega \in \{1, 2, 3\}$. Second, and more conclusively, the comparison between the fluctuating strain spectra under quiescent-background and wind-on conditions provides unambiguous evidence that the $St_\Omega = 3$ peak in the blade strain is of aerodynamic origin: this peak is entirely absent in the "wind-off" rotating baseline, where all mechanical, gravitational, and centrifugal forcing mechanisms are active but no (or negligible) aerodynamic interaction is present. Its emergence exclusively under "wind-on" conditions constitutes, by process of elimination, proof that the blade strain dynamics at $St_\Omega = 3$ are driven by aerodynamic interaction with the flow field in the turbine's wake, and not by inertial artifacts. Whether this coupling is driven by wake structures imprinting onto the blade, by blade motion modulating vortex strength as shown in [11], or by a co-evolving coupled system, does not alter this conclusion. We are currently carrying on for a more fluids-mechanics focused paper, where we delve on cross-correlating and fully exploiting the mechanistic events coupling this dynamical system. We retain the analysis of coupling directionality and causality for this dedicated study exploiting the full temporal statistics of the synchronised measurements.

4. It is assumed that the measured strain experienced by the wind turbine blade can be decomposed into gravitational, centrifugal, and aerodynamic strain-driven components, and that the impact of the former two can be obtained through calibration in a quiescent atmosphere. However, unless these experiments were done in a vacuum, spinning the rotor would still also induce aerodynamic forces, just for different angles of attack compared to $U_\infty = 2.8m/s$. The presented results do therefore not show the aerodynamic component, but part of the aerodynamic component. This should be corrected throughout the manuscript.

   We have modified the revised manuscript accordingly—see added discussion in the third paragraph of section 3.3. ("Blade strain under gravitational and centrifugal loading"). We chose not to modify this throughout the manuscript for the sake of simplicity. Even though a pure decomposition of the strain into aerodynamic component is not possible as the gravitational+centrifugal strain components measurements are contaminated by an aerodynamic component, it is important to highlight that this residual component is relatively small when compared to the aerodynamic component with "wind-on" conditions.

5. Error bars should be added to all figures that compare different cases (specifically 4b, 5, 11, 12, 13b, 18a+b) to allow for a proper discussion of differences. Also, it should be added what the errors of the hot-wire measurements are.

   The errorbars based on the measurement uncertainty have been added to the referred figures. Discussion on the errors and uncertainties affecting the hot-wire measurements has also been added to the Appendix B ("Constant Temperature Anemometry Measurements"). A detailed section 2.4. "Experimental protocol" was also added to the manuscript detailing how the error-bars exploring uncertainty of the measurements were obtained.

6. Ll. 268 "*At the same time, modifications of the flow features within the wake feed back into the structural response of the blades, as the inherent wake dynamics are imprinted on them (de Oliveira et al., 2025).* " The citation is for a cylinder in turbulent inflows and does not really match the written sentence. This should be stated clearly. Also, I am skeptical that the interpretation can be used 1:1 for a wind turbine wake, see points above.

   Note that the effect of wake dynamics is experienced upstream through pressure propagation in a cylinder, provided that the flow is incompressible. Once more, this is related with the previous discussion on the physical mechanisms driving $St_\Omega = 3$ dynamic forcing presented so far. At the velocities wind turbines run, we expect to see the same behaviour whereas flow structures and velocity dynamics have their imprint propagated upstream through pressure, by which they interact with the blades. The CPSDs show the presence of a coupling mechanism between the blade, and the wind turbine's wake, without suggesting causality - as discussed above. However, we decided to remove the statement from the paper, mainly because discussion provided up to this point does not support the aforementioned argument.

7. Figure 11/ ll. 355: most curves do *not* show a monotonic increase, this is only the case for ROOT-C and MIDSPAN-C. Also, particularly for the TIP, without error bars, the data is too scattered to draw conclusions.

   We agree the evolution of the curves is not purely monotonic - especially considering the variations across FST cases. However, note the clear general increase of Δ_s with the increase of λ. We have adapted the discussion of this section accordingly by removing "monotonic", and pointing out to the clear general increase with λ, removing the over-statement.

8. Figure 14/ discussion in ll. 445: The distributions at the tip are not heavy-tailed, they are pretty similar to the other positions. For better comparison, I suggest to add a Gaussian fit, preferably the same curve for all 9 sub-plots, so that deviations from a normal distribution are directly obvious.

   This section has been reconstructed to account for the comments from the second reviewer. The strain data was aggregated across a spanwise region of the blade, combining measurements from multiple sensor locations. Our power spectral density analysis demonstrates that the strain components at different spanwise locations, are exposed to different dynamics - for instance, the chordwise strain component is less exposed to $St_\Omega \in \{1, 2, 3\}$ dynamics as observed in figure 21 of the revised manuscript. When

aggregating these spatially distributed, weakly correlated signals, the Central Limit Theorem applies: the sum of multiple uncorrelated or weakly correlated random variables tends toward a Gaussian distribution, even if the individual signals are not themselves Gaussian.

We have revised the manuscript to include additional analysis showing PDFs of individual strain components (spanwise and chordwise) at specific blade locations (Figure 18 of the revised manuscript). This decomposed analysis reveals that the spanwise component under quiescent conditions exhibits the expected non-Gaussian PDF associated with purely periodic loading from combined centrifugal and gravitational effects especially observed at the root and low λ, while the chordwise component shows different behavior due to its distinct loading mechanisms. If the strain dynamics were purely governed by periodic loads arising from centrifugal+gravitational sources, the PDF of the fluctuating strain would be non-Gaussian instead. This is the case for $\lambda = 2$ as we show in the new figure 18, for the spanwise strain. As the aerodynamic contribution to the strain increases further, the PDFs approximate Gaussian-like behaviour. The previous aggregation of dynamics was smothering interesting features of blade dynamics, and we believe that this new analysis of the data added valuable content to the manuscript. We believe this additional analysis strengthens the interpretation and addresses your concern comprehensively. A Gaussian fit has been added to all 9 sub-plots as the reviewer suggested.

9. Figure 17: Add the spectra for U=0 for the three TSRs

   The following figure 2 of the rebuttal document presents the requested spectra for $U = 0$ m.s^{-1} for the three λ assessed.

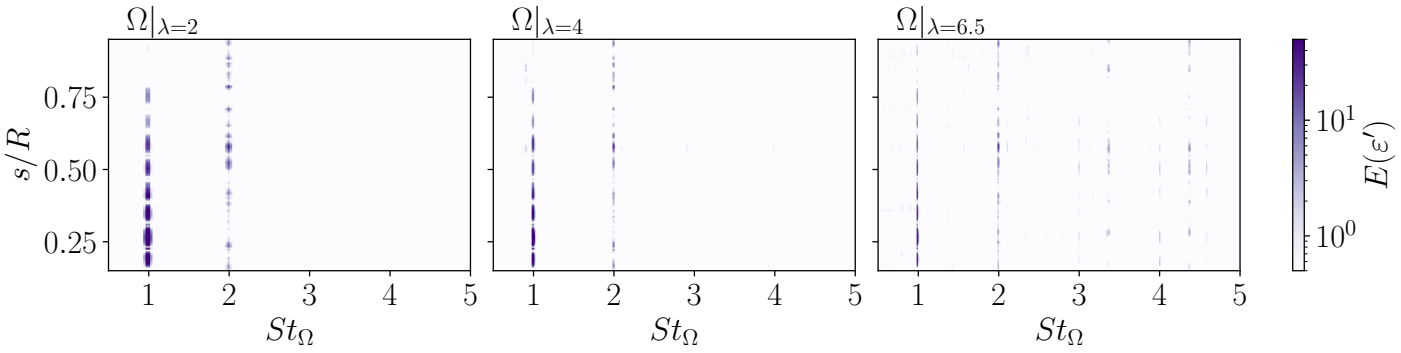

Figure 2: Power-spectral density of the fluctuating strain's response at selected λ.

   Similarly to the definition in the manuscript, $\Omega|_\lambda$ denotes an operating velocity that would match the rotational velocity of the corresponding λ.

   More importantly, figure 2 of the rebuttal provides definitive evidence that $St_\Omega = 3$ originates from aerodynamic conditions during "wind-on" conditions. Under quiescent conditions (U=0) at $\Omega|_{\lambda=4}$, the strain spectra shows no discernible peak at $St_\Omega = 3$. This peak emerges prominently only when the turbine is exposed to "wind-on" conditions, regardless of the FST "flavour", demonstrating unambiguously that it arises from aerodynamic interactions rather than from mechanical/resonance effects.

   It is important to note the increase in energy at $St_\Omega \in \{3, 4\}$ for $\widetilde{\Omega} = 6.5$ due to an increased relative velocity to the blade in line with the increased rotational velocity.

   This information has been added to the end paragraph of section 3.3. "Blade strain under gravitational and centrifugal loading" of the revised manuscript.

10. Figure 18:

    - 18 a) would be better comparable with b) if it was plotted over λ, too, and the downstream distance was color-coded.

      We agree with the reviewer's suggestion. The figure has been updated to the suggested layout. With the revision of the manuscript, the figure is now figure 22.

- For a) and b), have respectively the same axes ranges.

  We have opted to keep the different axis ranges to retain the dynamic evolution across each λ for the assessed St_Ω. However, we recognize that this may confuse the reader therefore, we now highlight the different y-axis ranges in the caption of the figure.

- 18b) C-St=1: the last point is not within the plot window.

  We appreciate the reviewer's observation. This has been fixed in the revised version of the manuscript.

11. Why are the results of case B only shown occasionally and not systematically?

    Results of case B have been omitted for the same reason results for all TSR tested were—to avoid repetitive results and discussion, and the inevitable increase of the length of the paper. Moreover, the conclusions drawn for case B are intermediate between case A and C. This was mainly done for the presentation of 2-D plots.

Minor comments:

1. References should be sorted according to their publishing year in the main part.

   We have carefully revised the manuscript and corrected this in its revised version.

2. Ll. 35: The citation is for a cylinder. This should be mentioned instead of suggesting that the study was done on an airfoil. There are more appropriate citations that investigate effects of freestream turbulence on the aerodynamics of blade sections, see for example [4] and references therein, or [11, 2] for an investigation of the impact of freestream turbulence on a tip vortex.

   We have decided to keep the citation as we intended to refer to the two possible effects of free-stream turbulence on blade loading - the direct and indirect as explained in the manuscript. However, to avoid confusion, we have clearly state in the reviewed manuscript that we are referring to work performed with a cantilevered cylinder.

3. Ll. 60 the statement would be true for ideal systems that do not have any delay before the control is acting, however, e.g. [8] show indirectly how much λ varies in normal operation.

   We appreciate the comment and have adapted the statement to account for the reviewer's point.

4. That increased FST breaks down tip vortices faster has been shown significantly earlier than 2023 (e.g., [1, 7]). Also, e.g. [9, 10, 5] argue more specifically that FST accelerates the transition to fully developed turbulent wakes in general ([1] for a wind turbine wake, [7] for porous disc wakes, [9] for cylinder wakes).

   We agree with the reviewer and have added the suggested citations to the reviewed manuscript.

5. Ll. 204: do you mean that the measurement time was 120s and the synchronized measurement started after the trigger?

   The synchronised measurement started after triggering, and lasted for 120s. We have clarified this in the revised version of the manuscript.

6. Figure 6: The color map is saturated in fig. 6a. The range should be expanded to 0 to show the homogeneity of your inflow.

   We have fixed this in the revised version of the manuscript - see now figure 11. Free-stream conditions are further explored in appendix A of the manuscript's revised version.

7. Figure 7: The forces are typically acting on the wing's quarter point. Also, the arrow marking U_{rel} does not reach the corner of the rectangle spanned by the induced velocities.

   We have fixed the schematic as suggested - see now figure 4.

8. Figure 15 and discussion: The broadening of the PDFs at $|y/R| < 0.4$ could also be due to turbulence from the nacelle, and that in the shear layers due to the higher TI levels in general - in accordance with Fig. 6. What type of intermittency are you referring to here? Adding more than 0 and -2 at the y-axis would be helpful.

   We thank the reviewer for this comment and have revised the manuscript accordingly - see also now figure 19 for the updated axis-ticks. The intermittency referred to here is associated with the blade operating condition rather than small-scale turbulence intermittency: at above-design operation the flow remains largely attached to the blades, resulting in a more coherent wake with reduced occurrence of large-amplitude velocity fluctuations, whereas at below-design operation flow separation and stall lead to a more incoherent wake and enhanced wake intermittency - the blade behaves closer to what a bluff body would behave in similar conditions. The discussion has been clarified to explicitly acknowledge the contribution of nacelle-induced turbulence near the wake centreline and increased turbulence levels in the tip-shear-layer regions.

9. L. 401 It looks like the references Biswas and Buxton, 2024b; Bourhis et al., 2025 are included as a reference to "tip vortices are shed from the blade tips" and not as a support for the fluctuating loads (which would be appropriate). If this is the case, I do not really see a reason for the addition here.

   We agree with the reviewer and have removed them from the revised manuscript.

10. Ll. 521 Add that this is due to the interaction of tip vortices through leap-frogging and add the appropriate references (e.g., [6] or [3]).

    We appreciate the comment, and have added the suggested discussion to the revised manuscript.

11. Ensure that you use the same notation for quantities throughout the manuscript. There are several examples where the axes labels (e.g., L_11, ε_a) and text/captions (e.g., L, ε'_a) are different.

    We appreciate the reviewer for pointing this out, and have carefully revised the manuscript to ensure the notation is consistent throughout.

Typos/etc.

1. L. 23 + corresponding reference: Porté-Agel.

   We have fixed this in the reviewed version of the manuscript.

2. eq. (2) t and τ are not defined.

   We have fixed this in the revised version of the manuscript.

3. L. 169 its

   We have fixed the typo in the revised version of the manuscript.

4. L. 401 reacting more strongly

   We have fixed the typo in the revised version of the manuscript.

5. L. 507 $\Gamma(\varepsilon'_a)$

   We have fixed this in the revised version of the manuscript.

6. L. 513 $\Gamma(\varepsilon'_a) = \Gamma(\varepsilon') - \Gamma(\varepsilon'_g)$

   We have fixed the typo in the revised version of the manuscript.

7. Fig. 1 - caption: please use SI units.

   The "$\mathbf{10'} \times \mathbf{5'}$" refers to the name of the wind tunnel used. We have kept the original sentence.

8. Fig. 6 ΔU undefined

   We appreciate the reviewer's observation. We have defined ΔU in the revised manuscript.

9. L. 325 compared to

   Corrected in revised manuscript version.

References

[1] S. Aubrun, S. Loyer, P. Hancock, and P. Hayden. Wind turbine wake properties: Comparison between a non-rotating simplified wind turbine model and a rotating model. *Journal of Wind Engineering and Industrial Aerodynamics*, 120:1–8, 2013.

[2] M. Coullouc, S. Yadala, G. K. Jankee, I. Neunaber, and R. J. Hearst. The effect of freestream turbulence on wing-tip vortex meandering and deformation. *International Journal of Heat and Fluid Flow*, 117:110013, 2026.

[3] M. Felli, R. Camussi, and F. D. Felice. Mechanisms of evolution of the propeller wake in the transition and far fields. *Journal of Fluid Mechanics*, 682:5–53, 2011.

[4] L. Li and R. J. Hearst. The influence of freestream turbulence on the temporal pressure distribution and lift of an airfoil. *Journal of Wind Engineering and Industrial Aerodynamics*, 209:104456, 2021.

[5] L. Li and R. J. Hearst. Effects of freestream turbulence on the wakes of circular and square cylinders. *Physical Review Fluids*, 10(11):114610, 2025.

[6] L. Lignarolo, D. Ragni, C. Krishnaswami, Q. Chen, C. S. Ferreira, and G. van Bussel. Experimental analysis of the wake of a horizontal-axis wind-turbine model. *Renewable Energy*, 70:31–46, 2014.

[7] T. Maeda, Y. Kamada, J. Murata, S. Yonekura, T. Ito, A. Okawa, and T. Kogaki. Wind tunnel study on wind and turbulence intensity profiles in wind turbine wake. *Journal of Thermal Science*, 20:1–8, 2011.

[8] P. Milan, M. Wächter, and J. Peinke. Turbulent character of wind energy. *Physical Review Letters*, 110(13):138701, 2013.

[9] I. Neunaber, M. Hölling, R. J. Stevens, G. Schepers, and J. Peinke. Distinct turbulent regions in the wake of a wind turbine and their inflow-dependent locations: the creation of a wake map. *Wind Energy*, 13(20):5392–5408, 2020.

[10] M. K. Vinnes, I. Neunaber, H.-M. H. Lykke, and R. J. Hearst. Characterizing porous disk wakes in different turbulent inflow conditions with higher-order statistics. *Experiments in Fluids*, 64:25, 2023.

[11] S. Yadala, S. Dehareng, I. Neunaber, et al. The effect of turbulence on a flexible finite wing: forces, deflections and the wingtip vortex. *Journal of Fluid Mechanics*, 1019:A38, 2025.